

Field Testing of Concrete Sleepers and Fastener Systems for the Understanding of Mechanistic Behavior

*J. Grassé, D. Lange, S. Wei, D. Kuchma
University of Illinois at Urbana-Champaign, Urbana, IL, USA;*

1. ABSTRACT

To adequately satisfy the demands placed on railway infrastructure through ever increasing freight tonnages in heavy haul operations, as well as the development of high speed rail, the design and performance of concrete sleepers and elastic fastening systems must be improved. This study encompasses a full-scale field test program to determine the parameters within the sleeper-fastener system necessary to conduct a mechanistic design. The test program utilized strain gauges, linear potentiometers, and matrix based tactile surface sensors (MBTSS). Testing was conducted on concrete sleepers utilizing varying fastening system designs at multiple heavy haul track locations. The testing has provided measurements of stresses in the concrete sleeper, rail seat, insulator, and fastener. The instrumentation strategy has also provided measurements of rail displacements in order to quantify the rigid body movement of the rail as it relates to various loading conditions and fastening systems. The data on loading and resultant behavior has been used to develop and validate simulated loads in laboratory testing and feed into a comprehensive analytical model. The synchronization of this data has also allowed for the quantification of vertical and lateral rigidity of the sleeper-fastener system. This study is part of a research program funded by the Federal Railroad Administration (FRA) aimed at improving concrete sleepers and fastening systems to withstand the loading conditions of increasing heavy haul and high speed rail traffic.

2. INTRODUCTION

Historically, in times of increasing freight tonnages and railroad traffic, concrete sleepers were used to replace traditional timber sleepers. Concrete sleepers provide superior durability and capacity, which allow them to outlast the standard timber sleeper in track with higher degrees of curvature and extreme weather conditions. Concrete sleepers also have the distinct advantage of improved track geometry retention, especially important in sustaining high speed rail and heavy freight lines. [1]

With the continuing increase in annual gross tonnages, concrete sleepers are experiencing a wide variety of failure mechanisms. In North America, the most common failure mode is rail seat deterioration (RSD): the wearing out of the concrete within the rail seat, often due to abrasion. [2] This abrasion is accelerated in the presence of water and in complex track geometry such as steep track grades and high degree curves. Concrete sleepers are also susceptible to flexural cracking, which often propagates from the center binding with diminished ballast support. Other components of the fastening system are also at risk of failure. Fatigue and abrasion of the fastening clips, shoulders, and insulators can allow for additional movement in the system and subsequent deterioration of other components.

In order to understand the mechanisms of the sleeper-fastener system, component behavior and system demands must be investigated. This includes an understanding of load transfer among each component. There is also a need for the magnitude of these input loads with respect to the train speed, car weight, track curvature, grade, and various fastening systems. [3] Obtaining these measurements synchronously will provide insight into the more complex interactions and

allow for a more purposeful, mechanistic design of the system and the field results to help create more practical design recommendations. [4]

In the pursuit of this mechanistic design, efforts have been made at the University of Illinois at Urbana-Champaign (UIUC) to formulate a comprehensive testing regime that can be implemented in operational track. The instrumentation plan includes the use of strain gauges (surface and embedment), linear potentiometers, and matrix based tactile surface sensors (MBTSS). The full-scale field test will provide measures of vertical and lateral load, rail and sleeper displacements, and stresses within the clip and insulator. This data will be investigated with resultant axle loads measured by the Transportation Technology Center, Inc. (TTCI) using an Instrumented Wheelset (IWS). The data will also be used to verify a comprehensive finite element model developed by UIUC to investigate the behavior of the sleeper-fastener system.

A preliminary test has been conducted in November of 2011 at the Transportation Technology Center (TTC) in Pueblo, Colorado, USA. The intent of the test was to test the feasibility of some of the instrumentation ideas and to prepare for future testing at TTC. Some results from this preliminary investigation are included in this paper. However, the bulk of our testing for the determination of the mechanistic behavior of the sleeper-fastener system will be conducted in TTC over the next years (tentatively July 2012, November 2012, and April 2013).

3. LOAD MEASUREMENTS

In order to obtain vertical and lateral loads, UIUC has chosen to use three configurations of strain gauges on the rail (Fig. 1). Because the rail is a slender, uniform member which remains in the elastic range and has homogenous material and geometric properties, it is optimal for deriving input loads from analysis of surface gauges.

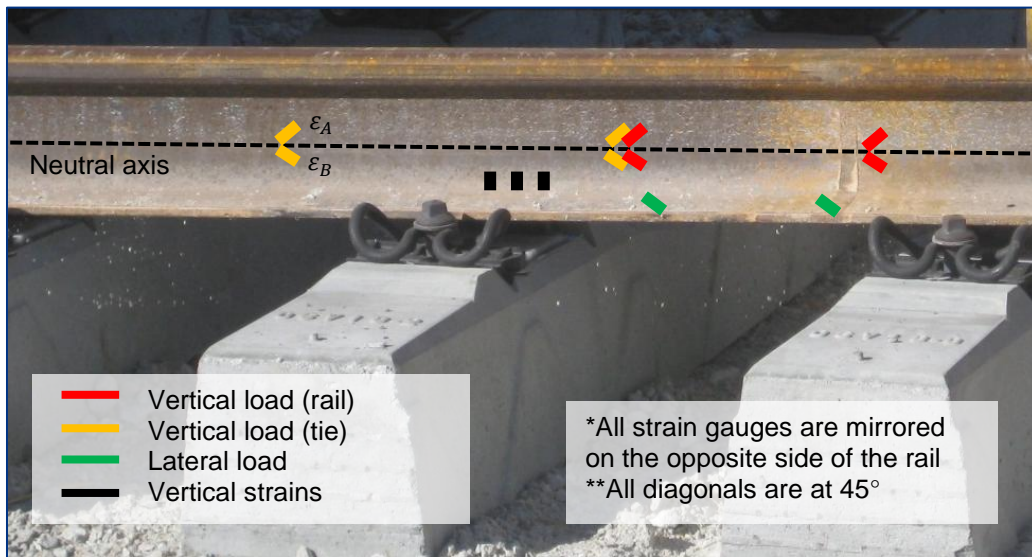


FIGURE 1: Configuration of strain gauges for attaining vertical & lateral loads.

In order to calculate vertical loads as they pass over the rail seat, one must know the shear force within the rail. The shear force [V] of one cross section of rail can be determined by:

$$V = \frac{EI}{(1 + \nu)Q} \epsilon_v$$

where E is the modulus of elasticity, I is the moment of inertia, ν is the Poisson's ratio, and Q is the first moment of area of the steel rail, and ε_V is the shear strain (absolute sum of strains measured 45° from the neutral axis). [5]

The shear strain can be determined from four strain gauges oriented 45° from the neutral axis on each side of the rail along one vertical plane. The shear strain is:

$$\varepsilon_V = (\varepsilon_A + \varepsilon_{A^*}) - (\varepsilon_B + \varepsilon_{B^*})$$

where the strains are designated in Fig. 1 (A^* and B^* denote mirrored strains on gauge side).

The vertical force, P , acting between two determined shear forces without any constraints within the two planes of interest is:

$$P_Z = \frac{EI}{(1 + \nu)Q} (\varepsilon_1 - \varepsilon_2) \propto (\varepsilon_1 - \varepsilon_2)$$

where ε_1 and ε_2 are the shear strains from two cross sections. Due to this proportional relationship between vertical and surface strains, a full Wheatstone bridge can be used and the strains summed to ratiometrically represent a quantifiable vertical load. Since it is difficult to determine the moment of inertia and area of the rail cross section, calibration can be done to associate output voltages to wheel-rail loads.

These strain gauge assemblies will be utilized in the crib between concrete sleepers that we intend on instrumenting. A 20 kip (89 kN) vertical load will be applied to the crib and a gain factor will be recorded. The patterns will also be utilized above a rail seat, with the vertical planes on either side of the concrete sleeper using the same gain factor. Since the concrete sleeper provides a reaction force, the output load would be a difference between the applied load and magnitude of load going into the rail seat.

Similarly, lateral loads can be measured from strain gauges on the rail base oriented 45° from the web. To calibrate the same 20 kip (89 kN) vertical load will be applied in addition to 10 kips (44 kN) of lateral force.

There are also additional vertical strain measurements that will be taken on the web near the base of the rail at adjacent sleepers ("Vertical strains" in Fig. 1). Either one or three gauges will be welded to each side of the rail. The average of the gauges on each side will provide a comparable representation of vertical loading, while the difference of strain on each side will provide a representation of lateral loading. These strain values will also be used to verify the finite element modeling work, and potentially, from correlating these values with the model, provide measurements of load.

4. DISPLACEMENT MEASUREMENTS

In order to characterize the loading condition within the sleeper-fastening system, it is imperative to know the movement of the components. The most integral movement that is most apparent and is a driving force for wear and abrasion is the rigid body movement of the rail. The magnitude of the movement is necessary in quantifying the lateral and vertical restraint of the system, while the way in which the rail translates and rotates is necessary in qualifying the behavior of the rail within the system.

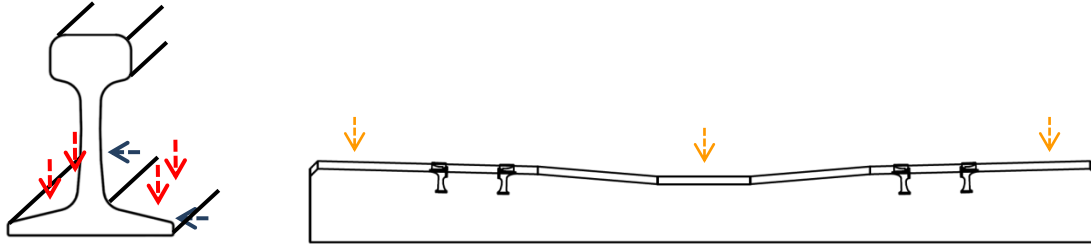


FIGURE 2: Vertical (red) and lateral displacements (blue) of rail; global displacements of the sleeper (orange).

To account for rail bending, measurements of lateral translation (transverse to the direction of the track) will be made at different heights of the rail profile. Most importantly, displacements will be measured at the rail base, rail head, and the neutral axis of the rail cross section. Supplemented with vertical displacement data, the lateral movement explains the extent to which the rail acts as bending beam or rigid body, which is as much a product of the fastening system as it is of the rail itself.

Global measurements of sleeper deflection will be made at 3 points along the sleeper. At each end as well as the center, vertical displacement will be measured using a long rod piled deep into the solid sub-strata. From these three measurements, the compression of the ballast can be determined. Also comparing relative displacement provides an understanding of the bending modes of the sleeper under heavy traffic loads. High sleeper displacements have also been associated with higher stiffness pads, which can be understood by using multiple rail pads and observing these global measurements alongside loading and displacement data. [6]

The rotations of the rail base in both principal directions above the rail seat can be quantified by measuring vertical displacements at four points over the rail seat (Fig. 2). The average of these points will provide a measure of vertical translation, from the compression of the rail pad assembly. They can be included with the sleeper displacement to understand the rail deflection, a significant indicator of track life, durability, and quality. [7] The difference of displacements from one side of the rail will provide a measure of rail bending along the length of the rail above the sleeper. The difference of displacements in the same location on the rail base on the field and gauge side will provide a measure of rocking that occurs due to lateral rotation.

5. INSTRUMENTED SLEEPERS

Thanks to one of our industry partners, L. B. Foster Company, eleven sleepers were instrumented with internal strain gauges and external surface gauges (Fig.3). These allow for the measurement of strains that demonstrate compression below the rail seat and flexure throughout the sleeper.

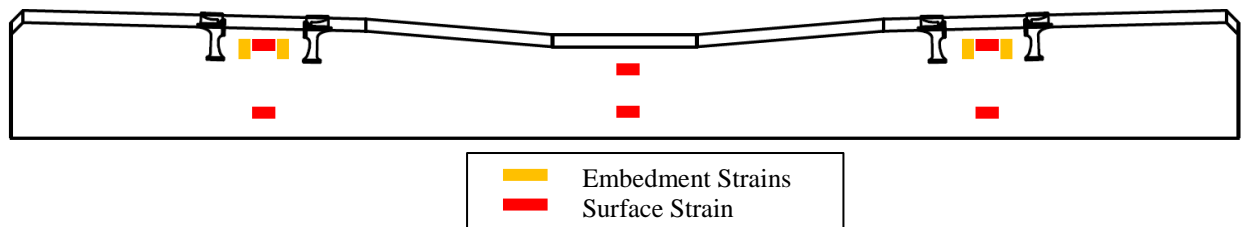


FIGURE 3: Configuration of embedment and surface strain gauges on concrete sleeper.

Embedment gauges were placed in a 2 x 2 matrix (3" x 2.5"; 7.6 cm x 6.4 cm), roughly 1.5" (3.8 cm) from the surface of the rail seat. The average of these strains will provide an understanding of concrete compression induced by vertical rail seat loads. The difference of strains in the two axes can give an idea of load attenuation through the rail pad and into the sleeper as well as a characterization of rocking and rotation due to an applied lateral load.

Using a static sleeper loading machine, which applies load to the rail seat, the embedment gauges were calibrated and strains were read at 0k (0 kN), 20k (89 kN), and 80k (356 kN); see Fig. (4). Due to the loading conditions (two wood planks between the rail seat and mechanical actuator); the compressive strains were slightly non-uniform. However, the average compressive strain of all the gauges produced a compressive strength (f'_c) of 6,900 psi (47.6 MPa), close to the manufacturer's estimate of a 7,000 psi (48.2 MPa) 24-hour strength.

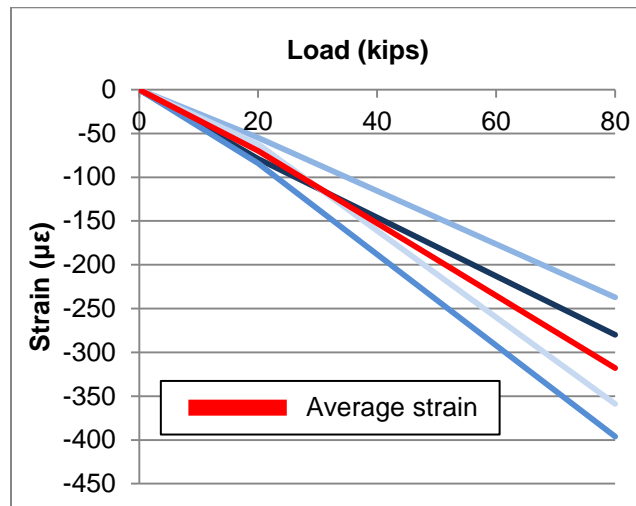


FIGURE 4: Calibration load-strain plot of embedment gauges, up to 80 kips (356 kN)

Surface gauges are used to measure the moments at critical sections of the sleeper: the rail seat area and center of sleeper. This will allow for the determination of flexural modes (up to our 3000Hz, used in data acquisition). The instantaneous moment [M] induced by a passing consist can also be calculated and expressed synchronously with our loading conditions:

$$M = \frac{(\varepsilon_2 - \varepsilon_1)}{d} EI$$

where ε_1 is the upper strain, ε_2 is the lower strain, and d is the vertical distance between the two gauges.

6. ADDITIONAL MEASUREMENTS

The rail requires electric isolation, commonly achieved by the use of a small nylon insulator, in order for a circuit-based track system to be used for traffic control. The mechanistic behavior of the insulators is important to understand within the sleeper-fastening system due to the high compressive forces that exist in the post. This produces a common failure mode, in which significant wear or complete fracture of the insulator can lead to further movement and deterioration within the system [8]. This mechanism is a product of shoving, or lateral translation of the rail. The insulator post is compressed between the rail base and the steel anchor.

Strain gauges are applied at the bottom surface of the nylon insulator with a small layer (0.1 in, 0.25 cm) of nylon shaved off to allow clearance for the gauges, leadwires, and protection (Fig. 5). Strain gauges will be oriented in the transverse direction of the railway track. Three gauges will be positioned at the center and 1 inch (2.5 cm) on each side, to give a compressive field.



FIGURE 5: Insulator post compression; location of strain gauges; direction of strain (left to right).

Strains from the clip and rail flange will also be measured synchronously with the full instrumentation plan to understand the movement and load transfer in the system and to feed into the finite element model. Strains will be measured on the rail base, an inch from the edge above the sleeper (Fig. 6). Strains will also be measured on the top surface of fastening clips to monitor the role of the clip in restraining the rail and to assure the component modeling adequately correlates to field measurements.

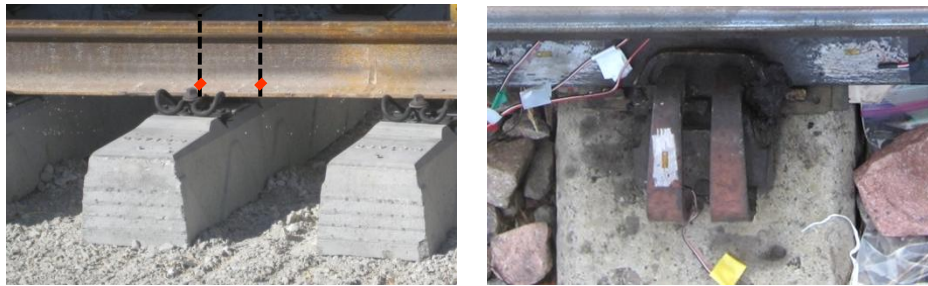


FIGURE 6: Location of transverse strain gauges on the rail flange; instrumented clip.

Clip strains were measured during train operations, as well as during the installation process to gain insight on the clamping force. A similar test was conducted on a 2 ft. (0.61 m) stick of rail, which was statically loaded at UIUC with a vertical load of 32.5 kips (145 kN) and lateral load of 16.9 kips (75.2 kN): a resultant force of 36.6 kips (163 kN) and L/V ratio of 0.52. The results are compared with a test run at TTC, using a measured axle load (Tab. 1).

TABLE 1: Stresses on the top surface of the fastening clip.

Stress on clip surface	Field [ksi/MPa]	Gauge [ksi/MPa]
After installation (TTC)	83/572	82/565
After loading (TTC)	95/655	65/448
Increase in clip stress	Load [kips/kN]	Gauge [ksi/MPa]
Wheel load (TTC)	44/196	+14.2/ +98
Static load (UIUC)	36.6/163	+7.8/ +54



At the lower speeds of 10 mph (16 km/h) and 20 mph (32 km/h), there was evidence of positive strain in both the clips, indicating a relaxation in the stressed clip, and consequently clamping force (Fig. 7). This was also evidenced in the static load test conducted at UIUC for field-side clips with low loads: up to about 15 kips (67 kN). There was no strain relief of the gauge-side clip in the controlled laboratory setup. It is important to note the rail seat investigated was in the high rail of a 5° curve track with a balance speed of 33 mph (53 km/h), and the runs that showed gauge-side clip relaxation were all underbalanced. Predominantly, however, the gauge-side clip always showed an increase in residual stress, while the field-side clip is nearly negligible. This suggests there is allotted rotation which works to uplift the gauge-side clip.

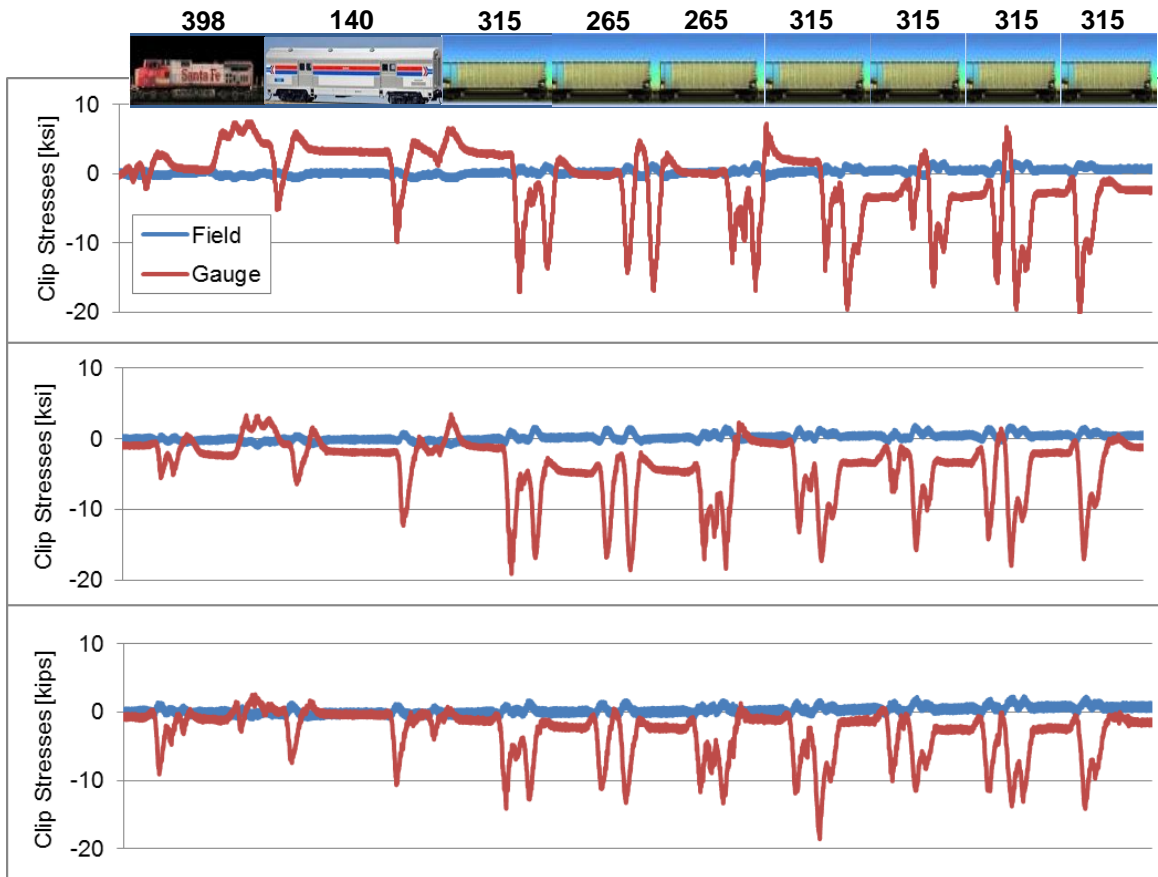


FIGURE 7: Stresses on the top surface of the clip, with the location and weight [kips] of the passing cars (10, 20, 40mph, top to bottom).

7. FULL-SCALE TESTING

Full-scale tests of the entire instrumentation plan will be conducted three times at TTC. The first trip will consist of two test regions where 15 new sleepers will be installed. One region will be in a tangent track, while the other will be on a curve of about 5°. Of the 15 installed sleepers in each region, the center 5 sleepers will be instrumented (Fig. 8), with heavy instrumentation being conducted on four rail seats (three adjacent rail seats and one on the opposite side of the center sleeper). The other rail seats will be partially instrumented with only vertical strains measured on the lower section of the web on the gauge and field side. Field tests are tentatively scheduled for July 2012, November 2012, and April 2013.

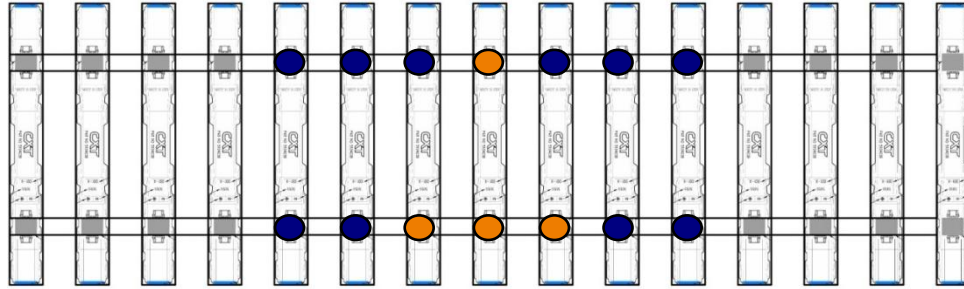


FIGURE 8: Locations of heavily instrumented (orange) and partially instrumented (blue) rail seats.

8. Acknowledgements

Funding for this research effort has been provided by the Federal Railroad Administration (FRA), part of the United States Department of Transportation (US DOT). The published material in this report represents the position of the authors and not necessarily that of DOT. We have also received generous support and guidance from our industry partners: Union Pacific Railroad; BNSF Railway; National Railway Passenger Corporation (Amtrak); Amsted RPS / Amsted Rail, Inc.; GIC Ingeniería y Construcción; Hanson Professional Services, Inc.; and CXT Concrete Ties, Inc., an LB Foster Company. We also thank Harold Harrison; Vince Peterson from CXT Concrete Ties, Inc.; Tim Crouch from the Monticello Railway Museum; Steve Mattson from VAE Nortrak North America, Inc.; and Riley Edwards, Marcus Dersch, Thomas Frankie, Jacob Henschen, Tim Prunkard, Darold Marrow, and Marc Killion from the University of Illinois for their work and guidance on this project.

9. REFERENCES

- [1] FIB, 2006. *Precast concrete railway track systems. International Federation for Structural Concrete (fib)*. Sprint-Digital-Druck. Stuttgart, Germany.
- [2] Zeman, J.C., *Hydraulic Mechanisms of Concrete Tie Rail Seat Deterioration*, M.S., University of Illinois at Urbana-Champaign, Urbana, Illinois, 2010.
- [3] Hanna, Amir, 1975. *Railway Track Research – Theoretical and Experimental*. Portland Cement Association 1975. Skokie, IL.
- [4] Sadeghi, J., 2008. *Experimental evaluation of accuracy of current practices in analysis and design of railway track sleepers*. *Canadian Journal of Civil Engineering*, 35 (9), pp. 881-893
- [5] Ahlbeck, D., M. Johnson, H. Harrison, R. Prause, 1976. *Pilot Study for the Characterization and Reduction of Wheel/Rail Loads*. U.S. Department of Transportation, Springfield, VA.
- [6] Johansson, A., Nielsen, J.C.O., Bolmsvik, R., Karlström, A., Lundén, R., 2008. *Under sleeper pads-Influence on dynamic train-track interaction*. *Wear*, 265 (9-10), pp. 1479-1487.
- [7] Anderson, J. S., & Rose, J. G., 2008. *In-situ test measurement techniques within railway track structures*. Paper presented at the *Proceedings of the ASME/IEEE/ASCE Joint Rail Conference, JRC 2008*, 187-207.
- [8] Lutch, R., 2009. *Capacity Optimization of a Prestressed Concrete Railroad Tie*, M.S., Michigan Technological University.